Wake-induced vibration of tandem cylinders of different diameters

Article *in* Journal of Fluids and Structures · October 2014

Impact Factor: 2.02 · DOI: 10.1016/j.jfluidstructs.2014.07.001

1 author:

Gustavo R S Assi
University of São Paulo
30 PUBLICATIONS **237** CITATIONS

Journal of Fluids and Structures 50 (2014) 329–339

Contents lists available at ScienceDirect

Journal of Fluids and Structures

journal homepage: www.elsevier.com/locate/jfs

Wake-induced vibration of tandem cylinders of different diameters

Gustavo R.S. Assi

Department of Naval Architecture & Ocean Engineering, University of São Paulo, NDF, Escola Politécnica, 05508-030 São Paulo, Brazil

ARTICLE INFO

Article history:
Received 3 February 2014
Accepted 2 July 2014
Available online 22 August 2014

Keywords:
Wake-induced vibration
Circular cylinders
Vortex wake
Flow interference

ABSTRACT

The wake-induced vibration (WIV) of the downstream cylinder of a tandem pair is investigated for different diameter ratios of $D_1/D_2 = 1/1$, 1/2 and 1/3, where D_1 and D_2 refer to the upstream and downstream cylinders, respectively. The streamwise separation between the cylinders was $L/D_1 = 3.5$, 7.0 and 6.5, respectively, measured from the centre of the upstream cylinder to the forward stagnation point of the downstream cylinder. Experiments with low mass-damping cylinders have been conducted in a water channel at around Re=25 000. The dynamic response showed that the downstream cylinder experienced WIV for all diameter ratios investigated, with displacement amplitudes reaching more than 1.5 diameters for higher reduced velocities beyond the vortex resonance range. The frequency response showed a similar behaviour for all three configurations, giving hints that a type of wake-stiffness mechanism might be governing the frequency of oscillation for all diameter ratios. The response was found to be dependent on both D_1/D_2 and L/D_1. In all cases, the static upstream cylinder was found to shed vortices as an isolated cylinder, not influenced by the presence or movement of the downstream body. Lift and drag coefficients as well as measurements of velocity fluctuations in both wakes are presented for all cases.

1. Introduction

When an elastic bluff body, like a circular cylinder, is immersed in the wake developed from an upstream body it will dynamically respond with *wake-induced vibrations* (WIVs). This hydroelastic mechanism has also been referred to as 'wake-induced galloping', 'interference galloping' or 'wake-displacement excitation' (Ruscheweyh, 1983; Bokaian and Geoola, 1984; Zdravkovich, 1988) and consists of the excitation of the downstream body by the interference of vortices developed in an unsteady wake generated upstream. The response of the downstream cylinder of a tandem pair is known to be severely increased by WIV when compared with that of an isolated cylinder under the resonant phenomenon of *vortex-induced vibration* (VIV).

Assi et al. (2010) reported on the effect of flow interference in the response of two identical cylinders aligned with the flow with centre-to-centre separations as large as 20 diameters. They have shown that vortices in the upstream wake play an essential role in driving the high-amplitude vibrations of the downstream cylinder. In fact, they performed an idealised experiment in which the unsteady vortex wake was replaced by a steady shear flow of equivalent mean velocity profile. They showed that the downstream cylinder immersed in that shear flow responded with a distorted type VIV but not with

E-mail address: g.assi@usp.br

http://dx.doi.org/10.1016/j.jfluidstructs.2014.07.001
0889-9746/

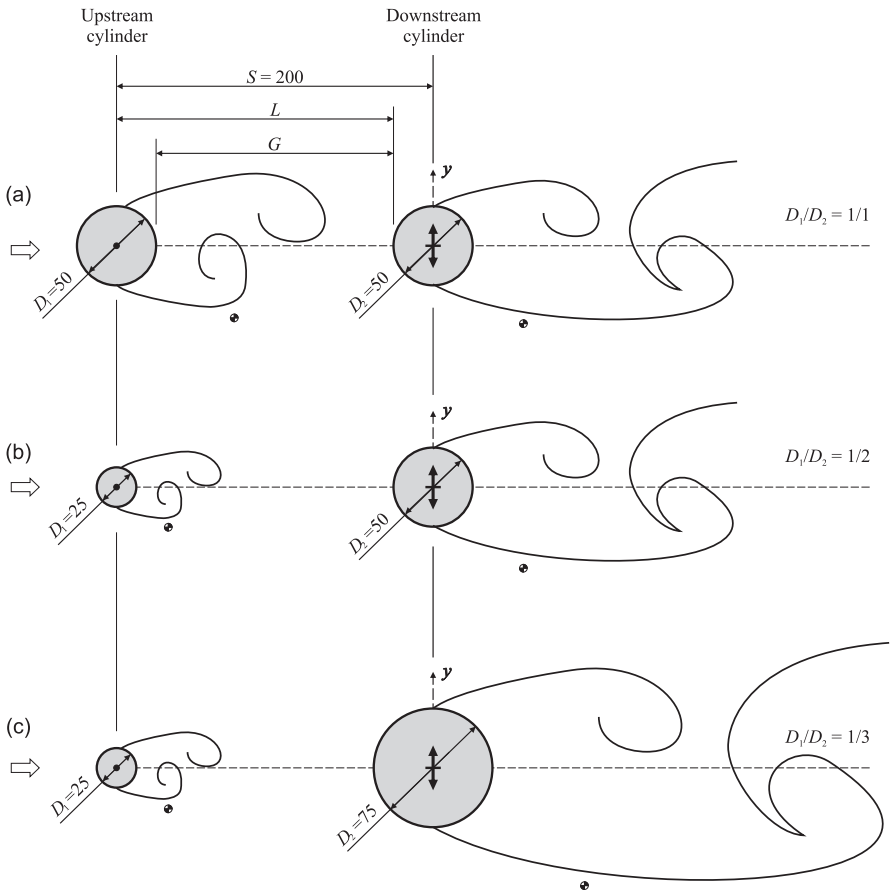

Fig. 1. Tandem configurations varying cylinders diameters. (a) $D_1/D_2 = 1/1$, (b) 1/2 and (c) 1/3. Dimensions are in millimetres. Sketches drawn to scale.

high-amplitude WIV. Their conclusion was that the unsteady interaction of coherent and periodic vortices from the upstream wake was necessary to input energy into the system and sustain the vibration.

The present work is a step further in the direction of understanding the vortex–structure interferences driving WIV of two bodies. This time we are concerned with varying the length and time scales of the wake involved in this kind of fluid–structure interaction. The downstream cylinder of a tandem pair is immersed in the wake developed from an upstream cylinder with smaller diameter. Consequently, the length and the time scales of the vortices that come from the upstream wake and reach the downstream cylinder vary proportionally. Three tandem configurations with the smaller cylinder positioned upstream are investigated in the present study, as illustrated in Fig. 1. The subscripts 1 and 2 will always refer to the upstream and downstream cylinders, hence D_1 and D_2 represent the respective cylinder diameters. Three diameter ratios of $D_1/D_2 = 1/1, 1/2$ and $1/3$ were chosen for the experiments and the centre-to-centre separation was kept constant at 200 mm in order to allow for the upstream wake to develop in the gap with no interference from the second body. As a consequence, the wake reaching the second cylinder will be proportionately different in each case due to the scale of the upstream vortex shedding mechanism and wake diffusion in the gap.

(*Note*: The subscripts in the non-dimensional numbers follow the same convention. Reynolds numbers (Re_1 and Re_2) take the diameter of the specified cylinder and Strouhal numbers are calculated employing the vortex shedding frequency (f_s) and the diameter of the referred cylinder, i.e. $\mathrm{St}_1 = f_{s1}D_1/U$ for the upstream cylinder and $\mathrm{St}_2 = f_{s2}D_2/U$ for the downstream cylinder.)

1.1. Flow interference between cylinders

Zdravkovich (1988) proposed a map of wake interference for two static cylinders with the same diameter arranged in several tandem and staggered configurations. The boundaries for each wake-interference zone clearly depend on the diameter of the two cylinders involved. It is expected that a smaller cylinder in the wake of a larger one will have to move many diameters across the wider wake before being free from any flow interference from upstream. The opposite might also happen for a larger cylinder moving across the narrower wake of a smaller body; the wake-interference zone might be reduced. Hence, the wake-interference map proposed by Zdravkovich (1988) will probably be different for each diameter

ratio illustrated in Fig. 1. However, this thought exercise might only be valid for the wake-interference of two static cylinders. Based on the results of Assi et al. (2010) we expect minute vortex impulses from upstream to have a considerable effect on the excitation of the downstream cylinder, especially if it presents low structural mass and damping. Even the wake of a smaller cylinder placed upstream (with smaller vortices at a higher frequency) might be sufficient to induce severe WIV of the second larger body. Assi (2014) showed that the flow interference from the upstream wake will have an effect even if the downstream cylinder is initially positioned further out of the centreline of the wake, in what is called a staggered arrangement. An effect on the response of the downstream cylinder was observed for lateral separations up to 3 diameters when $S/D=4$ (both cylinders having the same diameter).

Most of the studies concerning interference of cylinders with different diameters are focussed on the effect that the wake of a smaller cylinder has on the flow behaviour around a larger body. Studies of this kind can be classified as flow control experiments and some will go as far as to consider both the small and large cylinders as a coupled pair able to respond to flow-induced vibrations. Rahmanian et al. (2012) performed numerical simulations of the flow around two interfering cylinders with $D_1/D_2=0.1$. The pair was mechanically coupled and able to respond to flow-induced vibrations in two degrees of freedom, thus the investigation was aimed at understanding the interference effect of the smaller cylinder on the larger one as the gap and the angular position were varied between them. Their main finding was that the maximum vibration observed for the coupled pair occurred when the cylinders were arranged in staggered configuration and not aligned with the flow. Tsutsui et al. (1997) also presented an experimental and numerical investigation employing a similar arrangement of a very small cylinder positioned about the main body. But their investigation with static cylinders only showed that the wake structure and fluid forces were strongly affected by the position of the small cylinder. Zhao et al. (2005) and Zhao and Yan (2013) both presented numerical investigations in the same lines.

The present investigation, however, is not concerned with the flow interference between a very small cylinder positioned in the vicinity or about a main body nor it is concerned with a mechanically coupled pair. In the present work we will investigate the flow interference from a fully developed upstream wake on the response of the downstream cylinder of a tandem pair with relatively similar diameters. Thus, we are truly concerned with the effect that wakes of different scales will have on the wake-induced vibration of the downstream body. The upstream cylinder is always static and only responsible for generating a vortex wake that reaches the second body. The downstream cylinder is free to respond with flow-induced vibrations only one degree of freedom (1-dof) in the cross-flow direction. The in-line separation between the cylinders is kept constant at all times.

In our experiments, the upstream cylinder is always smaller than the downstream one. Nevertheless, it is worth mentioning the work done by Huang and Sworn (2011), in which they investigated the WIV of a cylinder when a lager body was placed upstream. In their experiments, performed in a water flume at subcritical Re, they employed a pair of rigid cylinders in tandem with $D_1/D_2=2.0$ and in-line spacing varying between $S/D_1=1$ and 10. Both cylinders were elastically supported in a low-damping system, free to respond in both the cross-flow and streamwise directions. They observed that the signature of lift measured on the downstream cylinder had the frequency components from the upstream vortex shedding as well as from its own vortex shedding, with predominance depending on the in-line spacing. Independently of the separation, they observed that the upstream cylinder always showed a typical VIV response, while the downstream cylinder presented WIV response reaching cross-flow displacements as high as 1.5 diameters in amplitude. In a later study, Huang and Sworn (2013) employed cylinders with $D_1/D_2=1$, 2 and 4 and varied the in-line spacing between $S/D_1=1$ and 15 to reach similar conclusions. As expected, when both cylinders were held static, the average drag measured on the downstream cylinder showed the effect of a slower mean flow coming from the upstream body, which in turn was dependent on the diameter ratio and the in-line separation.

Alam and Zhou (2008) performed wind-tunnel experiments with a pair of static cylinders with different diameters to measure forces and flow structures of the interfering flow. The diameter ratio varied between $D_1/D_2=0.24$ and 1.0 and the in-line spacing was fixed at $L/D_1=5.5$, providing that a fully developed wake was generated in the gap for the range of $Re_2=0.6\times10^4$–2.7×10^4. The authors found two distinct frequencies of vortex shedding coexisting in the wake downstream of the pair, which were attributed to the vortex shedding mechanisms of each of the cylinders. This was only verified for certain diameter ratios for static cylinders.

In a recent study, Alam and Zhou (2014) investigated the flow-induced response of a similar pair of cylinders at $Re_2=2.7\times10^4$. The smaller, static cylinder was placed upstream of a cantilevered cylinder, with the ratio between the two diameters also varying between $D_1/D_2=0.24$ and 1.0. This time the tandem cylinders were arranged in close proximity, with in-line separation being set at $L/D_2=1.0$ and 2.0. Interestingly, Alam and Zhou (2014) only observed severe vibrations of the downstream cylinder for $D_1/D_2=0.24$–0.8 (considering both in-line separations tested) and not for cylinders with the same diameter. In addition, vibrations were observed for reduced velocities in the range of 13–22.5, too high to be regarded as a result of resonant VIV. They explained that the smaller cylinder placed upstream would generate a narrower wake capable of exciting vibrations as the shear layers flipped from one side to the other during the cross-flow displacement of the downstream body. For cylinders of equal diameters at close proximity, on the other hand, the wider upstream wake would engulf the downstream cylinder making the side-to-side flipping mechanism rather difficult to occur. We believe these vibrations are better described by the 'gap-flow switching' mechanism explained in Zdravkovich (1988), since the close proximity of the bodies prevents a developed wake to form in the gap. The fact that the downstream cylinder was mounted as a cantilever may result that not its entire length is being excited by the same mechanism, especially knowing that 'gap-flow switching' requires a considerable amount of transverse displacement to occur.

2. Method

At first sight it seems rather simple to find a parameter to represent the in-line separation between the cylinders, but one must not be mistaken by the effect that the apparent simplicity of the geometries in Fig. 1 has on the hydrodynamic mechanisms involved. Since both cylinders vary in diameter, the effective gap between the bodies changes from case to case. For example, to consider the centre-to-centre separation S to be the characteristic in-line distance of the problem will make the gap between cylinders in Fig. 1(b) to appear larger than in the other two cases. Another way to interpret the actual length scale affecting the flow interference would consider the gap G measured between the cylinder walls, thus making the cylinders in Fig. 1(a) to look closer than the others. One can see that there are several ways to organise and interpret the data. The physical characteristics of the wake interference phenomena must not be forgotten. On top of that, there is the problem of choosing which diameter should be the reference for normalisation: that of the static upstream cylinder (D_1), where the wake is generated, or that of the oscillatory downstream cylinder (D_2), the object of WIV.

Perhaps the most reasonable interpretation would consider the distance measured from the centre of the upstream cylinder to the wall (or forward stagnation point) of the downstream cylinder, defined by L in Fig. 1. Such an interpretation might be possible because the separation points on the upstream cylinder are practically aligned with the centre of the cylinder; hence at roughly the same location for all three configurations independently of the dimension D_1. The interference effect of the wake on the downstream cylinder, on the other hand, depends on D_2 and the position of the forward stagnation point. Therefore, as far as wake interference is concerned, the most appropriate parameter to be employed in the study appears to be L/D_1, non-dimensionalised by the diameter of the upstream cylinder, where the upstream wake is being generated.

Table 1 presents all geometrical parameters and respective normalisations as explained in the paragraphs above. All possible normalisations of S, G and L were kept in the table to illustrate the variety of ways that could be employed in interpreting the in-line separation. In the present work, however, L/D_1 is considered to be the length scale representative of the wake interference phenomenon, thus special attention will be given to the penultimate column.

2.1. Experimental setup

Experiments were performed during a test campaign in the Department of Aeronautics at Imperial College, London. Tests were carried out in a recirculating water channel with a free surface and a test section 0.6 m wide, 0.7 m deep and 8.0 m long. Flow speed was continuously variable up to $U=0.6$ m/s and free stream turbulence intensity was around 3%. Circular cylinder models were made from acrylic tubes, giving a maximum Re$=30\,000$ based on a cylinder diameter of 50 mm.

The downstream cylinder was fixed at its upper end to a 1-dof elastic mounting represented in Fig. 2. The model was aligned in the vertical direction passing through the free surface and mounted such that there was a 2 mm gap between the

Table 1
Geometrical parameters for the tandem configurations illustrated in Fig. 1. Dimensional terms in columns 2–6 are in millimetres.

D_1/D_2	D_1	D_2	S	G	L	S/D_1	S/D_2	G/D_1	G/D_2	L/D_1	L/D_2
1/1	50	50	200	150	175	4.0	4.0	3.0	3.0	3.5	3.5
1/2	25	50	200	162.5	175	4.0	4.0	6.5	3.25	7.0	3.5
1/3	25	75	200	150	162.5	8.0	2.7	6.0	2.0	6.5	2.17

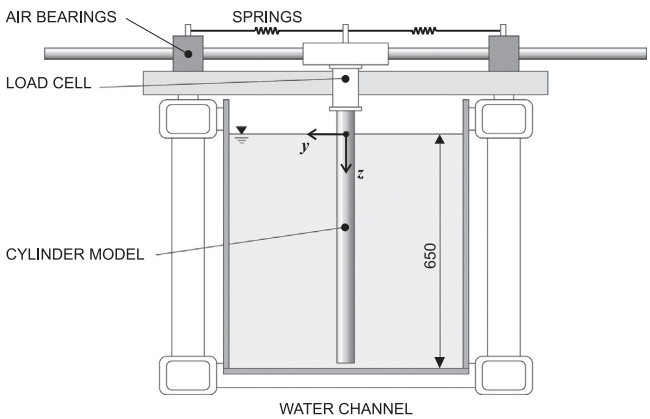

Fig. 2. Representation of the downstream cylinder mounted on the 1-dof rig in the test section of the water channel. View of the cross-section. Dimensions are in millimetres.

Table 2
Structural properties for the downstream cylinder.

D_1/D_2	m^*	$\zeta(\%)$	$m^*\zeta$
1/1	2.6	0.35	0.0091
1/2	2.6	0.35	0.0091
1/3	1.2	0.35	0.0041

lower end of the cylinder and the floor of the test section. It was judged preferable not to install end plates on the cylinder in order not to increase the fluid damping in the system. The support was firmly attached to the channel structure and sliding cylindrical guides were free to move in the transverse direction (y-axis) through air bearings. A pair of coil springs connecting the moving base to the fixed supports provided the restoration force for the system.

It is known that the dynamic response of a cylinder is extremely sensitive to the structural characteristics of the system; therefore extra care was taken to determine the precise value of natural frequency, mass and damping of the structure. The air bearings proved to be an effective way to reduce damping without compromising the stiffness of the structure, especially in resisting drag loads for higher flow speeds. By carrying out free decay tests in air it was possible to estimate the natural frequency (f_0) and the structural damping parameter of the system (ζ, calculated as a percentage of the critical damping). They are presented in Table 2 along with the mass ratio (m^*, calculated as the total mass divided by the mass of displaced water), for the configurations tested.

A load cell was installed between the model and the platform to measure hydrodynamic forces acting on the cylinder (inertial components have been subtracted from the total force acquired by the load cell). An optical positioning sensor measured the y-displacement without adding damping. Two hot-film probes were employed to measure velocity fluctuation in the wake of both cylinders in order to capture the frequency of vortex shedding close to the vortex formation regions. Probes were positioned at roughly $1D$ downstream of the cylinder centre and $1D$ to the side of the centreline; locations are marked by quartered-circle symbols in Fig. 1. More details about the apparatus, flow quality, design of the load cell and operation of the 1-dof rig can be found in Assi (2009).

Measurements were made using one set of springs and the reduced velocity range covered was from $U/D_2f_0 = 2$ to 30, where reduced velocity is defined using f_0 measured in air. The only flow variable changed during the course of the experiments was U, which alters both the reduced velocity and the Reynolds number. Throughout the study, cylinder displacement amplitudes ($\hat{y}/D_2$) were found by measuring the root mean square (r.m.s.) value of response and multiplying by $\sqrt{2}$ (the so-called harmonic amplitude). Displacements were non-dimensionalised by dividing by the downstream cylinder diameter.

3. Results and discussion

Fig. 3 presents the WIV response for the tandem configurations versus reduced velocity. Displacement and frequency curves are compared with the response of a single cylinder with $D=50$ mm, which will serve as a reference for the discussion that follows. During the typical single-cylinder VIV excitation, as U increases, the frequency of vortex-shedding (f_s) gets close enough to the body's natural frequency of oscillation (f_0) in a way that the unsteady pressure fluctuation in the near wake induces the body to respond in resonance. Once the cylinder starts to oscillate, high-amplitude movements will control the vortex formation and f_s will be *locked in* the response frequency (f) near f_0. If U continues to increase the typical vortex-shedding frequency will move far away from the natural frequency of the system, i.e. f_s and f will be uncoupled again. Refer to Bearman (1984) and Williamson and Govardhan (2004) for a detailed description of the VIV mechanism and typical responses.

Since reduced velocity was increased by changing U in the channel an extra horizontal axis has been introduced to indicate the equivalent Reynolds number scale calculated for a cylinder with $D=50$ mm. All three experiments were performed until the maximum flow speed was reached in the channel, making the third dataset look shorter in the reduced velocity scale; hence the Re scale is not true for the $D_1/D_2 = 1/3$ curve.

Fig. 3(a) presents the harmonic amplitude of vibration of the downstream cylinder. It is evident that all three configurations present the build-up of displacement for higher reduced velocities that are characteristic of WIV. For $U/D_2f_0 = 4$–7 all tandem configurations present a local peak of vibration related to the resonance of vortex shedding; this is equivalent to the upper branch registered for the single cylinder under VIV. But for $U/D_2f_0 > 12$ it becomes clear that the responses are not driven by resonance any longer, but sustained by the WIV mechanism.

The case $D_1/D_2 = 1/1$ (with $L/D_1 = 3.5$) reaches a maximum $\hat{y}/D_2 = 1.8$ at $U/D_2f_0 \approx 30$. For $D_1/D_2 = 1/2$ the maximum response reaches $\hat{y}/D_2 = 1.3$ at around the same reduced velocity, but the effective separation is now $L/D_1 = 7.0$, twice as much as the previous case. Between the first two cases there is no variation of Reynolds number, so the decrease in the level of response must be related to decreasing the diameter ratio and/or doubling the effective in-line separation.

On the other hand, when the diameter ratio was made even smaller in the $D_1/D_2 = 1/3$ configuration the response increased when compared with the $D_1/D_2 = 1/2$ case. A maximum $\hat{y}/D_2 = 1.4$ was reached for the maximum reduced

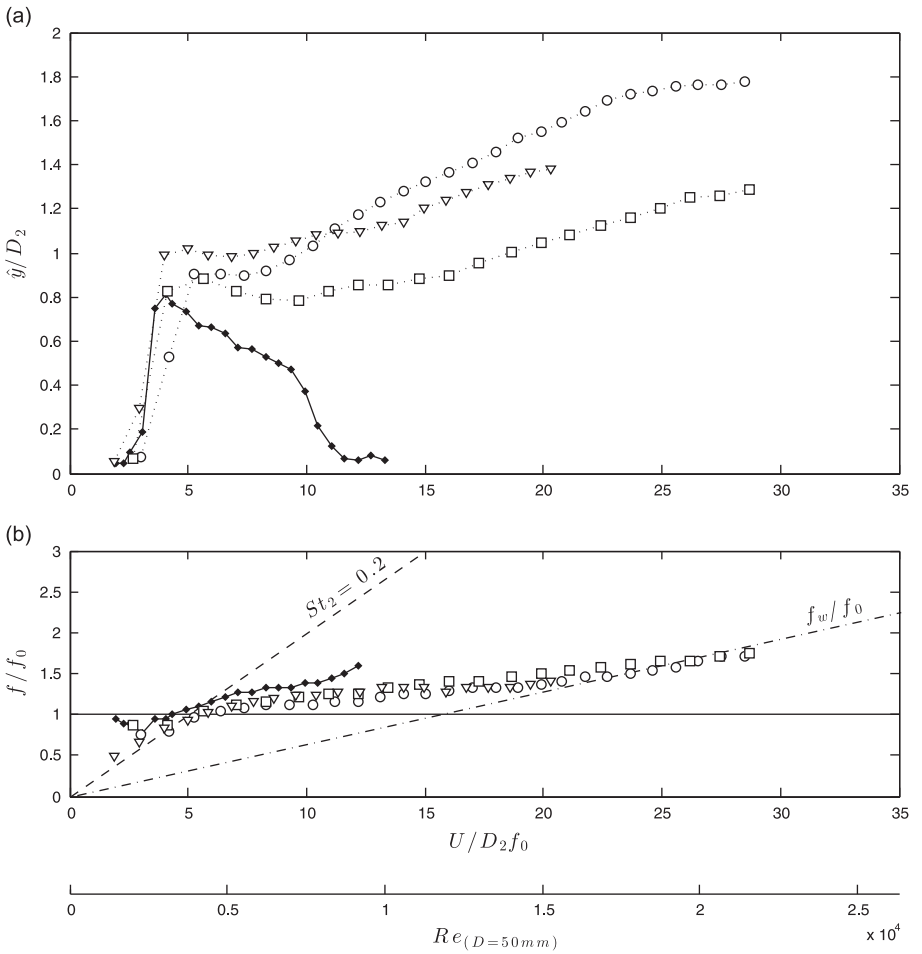

Fig. 3. WIV response of cylinders with different diameters. (a) Displacement and (b) frequency of vibration versus reduced velocity. Key: ♦, single cylinder VIV; ○, $D_1/D_2 = 1/1$; □, $D_1/D_2 = 1/2$; ▽, $D_1/D_2 = 1/3$.

velocity, now just above 20, but an amplification of the response was clear to be occurring for the whole range of reduced velocities tested. In this case, decreasing D_1/D_2 produced stronger vibration of the downstream cylinder, which might be related to the fact that the effective in-line separation decreased to $L/D_1 = 6.5$ when compared with the previous tandem configuration (it must be noted that Rehas also increased).

Comparing the three response curves in Fig. 3(a) we may conclude that both the diameter ratio and the effective in-line separation have a strong effect on the WIV response of the downstream cylinder. Nevertheless it is interesting to note that even the smallest upstream cylinder with $D_1/D_2 = 1/3$ is capable of inducing vibrations on the downstream body of comparable amplitude as a configuration with cylinders with equal diameters.

The mass ratio, however, might still be another factor playing some role in the amplification of response from case $D_1/D_2 = 1/2$ to 1/3. As seen in Table 2, the $D_1/D_2 = 1/3$ case presents $m^* = 1.2$, less than half of the $m^* = 2.6$ for the other two configurations due to the larger diameter of the cylinder. Probably a relatively lighter cylinder would be more vulnerable to the upstream excitation even though it comes from a much smaller cylinder. This could produce higher amplitudes of response during the VIV resonance range, as it is known to occur for a single-cylinder VIV. Past the VIV range, say for reduced velocities above 15, the response for $D_1/D_2 = 1/3$ is lower than that for $D_1/D_2 = 1$. We suspect this is related to the width of the upstream wake relative to D_2. In this case, the downstream cylinder moves out of the upstream wake at smaller displacements and the unsteady excitation mechanism proposed in Assi et al. (2010) is therefore weakened.

The dominant frequency of response of the downstream cylinder normalised by the natural frequency of vibration (f/f_0) is presented in Fig. 3(b). An inclined dashed line indicates that the frequency associated with the vortex shedding of the downstream cylinder was it to follow a typical Strouhal number of 0.2. Between $U/D_2f_0 = 2$ and 7, in the region associated with the stronger VIV resonance, all configurations vibrate with dominant frequency following close to the $St_2 = 0.2$ line, as well as the single cylinder under VIV. As flow speed is increased towards the end of the VIV synchronisation range, the dominant frequencies for all cases depart from the $St_2 = 0.2$ towards the horizontal line of $f/f_0 = 1$. Eventually, for even higher reduced velocities past the VIV influence, the frequency curves tend towards another dot-dashed line identified as

f_w/f_0. Surprisingly, this line represents the frequency of *wake stiffness* introduced by Assi et al. (2013) as the characteristic WIV frequency of vibration of the downstream cylinder of a pair with equal diameters. (Note that the slope of this line was determined in Assi et al., 2013 and is only valid for $D_1 = D_2$.)

The wake-stiffness concept explains that there is a natural frequency of oscillation of hydrodynamic nature (f_w) dominating over the response of the cylinder immersed in the upstream wake (Refer to Assi et al., 2013 for details on the estimation of f_w). We believe f_w to be strongly dependent on the vortex interaction occurring in the wake, thus depending on the width of the upstream wake as well as the length and time scales of the vortices being shed (wake topology). Tandem pairs with different diameter ratios would probably produce different values of f_w, but this was not measured in the present investigation. What is surprising here is that the frequency of response for $D_1/D_2 = 1/2$ was not expected to follow the f_w/f_0 line previously determined for $D_1/D_2 = 1/1$, but as a matter of fact it falls very close to it. Unfortunately the response curve for $D_1/D_2 = 1/3$ does not go much further than $U/D_2f_0 = 20$, but up to that point it follows the other two curves pretty well. If wake stiffness is a function of wake topology and geometry, as believed, it is not a strong dependency as to make significant difference in these response curves, at least not in the present range of D_1/D_2 and L/D.

In summary, even with considerable variations of D_1/D_2, L/D_1 and m^* the frequency signatures of WIV for all tandem cases are remarkably similar and follow very closely the behaviour governed by the wake stiffness of WIV introduced by Assi et al. (2013) for $D_1 = D_2$. More striking is the fact that the dominant frequency of vibration of the downstream cylinder is higher than the structural natural frequency of the system (line for $f/f_0 = 1$), clearly different from the expected vortex shedding frequency of the cylinder (line for $St_2 = 0.2$) and probably very different from the expected shedding frequency of the upstream cylinder, which has a smaller diameter. In order to clarify that, we shall turn to the frequency signature measured in both wakes and derived from the forces acting on the cylinders.

3.1. Frequency signatures of lift and wakes

Fig. 4 presents a series of contour plots representing the power spectrum signature of wakes and forces for the configuration $D_1/D_2 = 1/1$. Each plot shows the frequency scale non-dimensionalised by f_0 in the vertical axis versus reduced velocity in the horizontal axis. The intensity of the colour shade represents the power content for either velocity fluctuation in the wake or fluctuating force on the cylinder. Power spectra were normalised for each reduced velocity in order to make it possible to follow through branches of dominant frequency along the horizontal axis. The dominant frequency of oscillation presented in Fig. 3(b) is repeated as data points in each plot as a reference of the response.

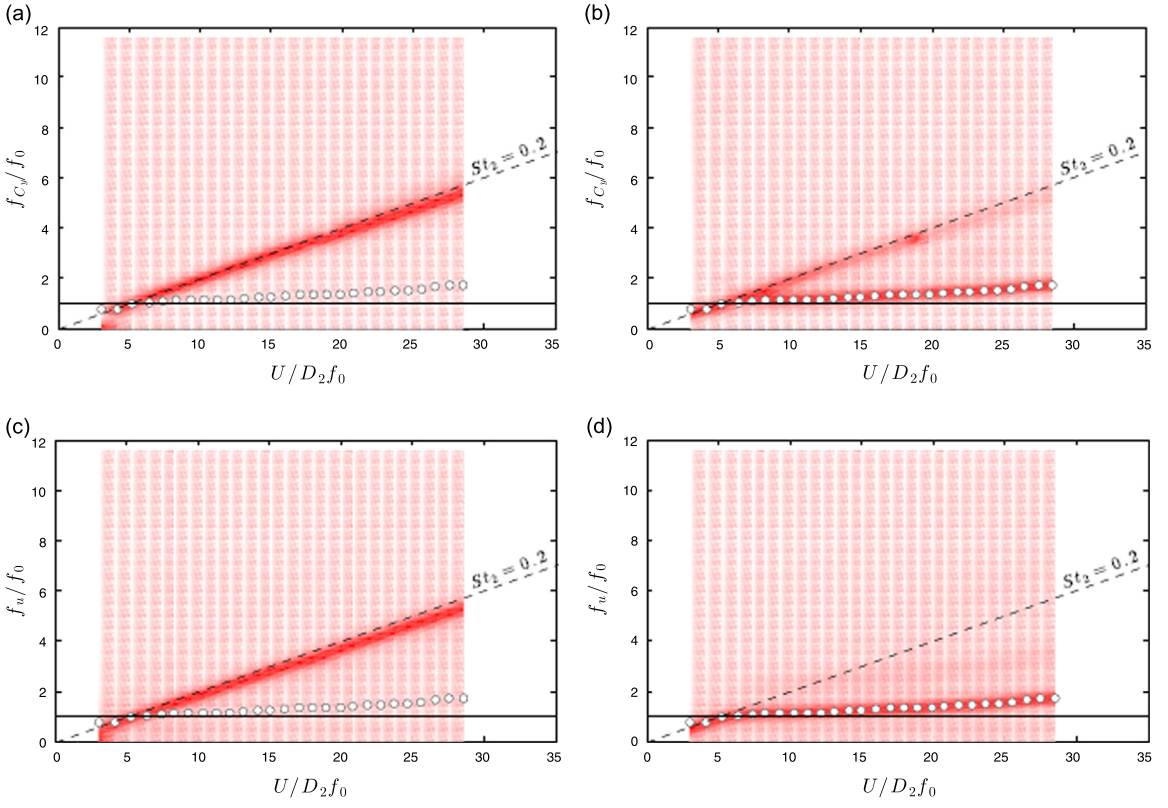

Fig. 4. Power spectra for configuration $D_1/D_2 = 1/1$. Frequency of lift on the (a) upstream and (b) downstream cylinders. Frequency of velocity fluctuation in the wake of the (c) upstream and (d) downstream cylinders.

The frequency signature of lift measured on the upstream cylinder (f_{C_y}/f_0) is presented in Fig. 4(a), revealing that the upstream static cylinder is shedding vortices as an isolated cylinder following the typical $St_2 = 0.2$ dashed line (in this case $D_1 = D_2$). As seen in Fig. 4(c), the behaviour is confirmed by the signature of velocity fluctuation in the wake (f_u/f_0) measured by a hot-film probe downstream of the upstream cylinder. Hence, the upstream cylinder is shedding vortices as an isolated cylinder and no traces of the frequency of oscillation of the downstream cylinder are noticeable in the spectra of the wake or lift.

The spectrum of lift (f_{C_y}/f_0) on the downstream cylinder, presented in Fig. 4(b), reveals that the second body indeed experiences lift at the frequency of shedding coming from the upstream cylinder. This is a result of vortices impinging on the downstream cylinder as it moves across the wake. However, a much stronger branch appears to dominate the spectrum, one which is associated with the frequency of vibration represented by the data points. Now, one cannot tell how much of the power in that strong branch is a result of the unsteady flow excitation or simply the hydrodynamic inertia measured by the load cell as the cylinder moves across the wake. Perhaps it is a combination of both. A branch at that frequency would also appear if the cylinder were vibrating with f in still water. The fact is that this is the preferred frequency of vibration for the downstream cylinder, the one associated with the wake stiffness. This happens to be the only frequency branch identified in the wake of the downstream cylinder, as seen in Fig. 4(d), and no traces of vortex shedding following the Strouhal line were registered. Again, this might be the effect of the movement of the downstream cylinder dominating over the velocity fluctuations measured by the hot-film probe in the wake.

Moving on to the $D_1/D_2 = 1/2$ configuration presented in Fig. 5, we notice that the frequency signature of lift on the downstream cylinder (f_{C_y}/f_0), shown in Fig. 5(a), also presents a clear dominant branch coinciding with the frequency of oscillation, as expected. Other secondary frequency branches, nonetheless, can be seen to occur at the shedding frequencies of both cylinders, i.e. following the $St_1 = 0.2$ and $St_2 = 0.2$ dashed lines (represented by very light shades of colour in the contour plots). Looking at the wake signature of the upstream cylinder in Fig. 5(b) it becomes clear that the first body is shedding vortices as an isolated static cylinder and no significant traces of the downstream oscillation are being propagated upstream either. Once more, the wake signature (f_u/f_0) of the downstream cylinder in Fig. 5(c) only captures weak traces of these higher frequencies, with the dominant frequency branch being associated with the frequency of vibration. As noted before, Alam and Zhou (2008) verified the existence of higher frequencies associated with the upstream shedding for two static cylinders. We believe that when the downstream cylinder is free to oscillate the frequency of oscillation will dominate over the shedding frequencies of the upstream body and the latter will not be very clear in the spectrum plots of the downstream wake.

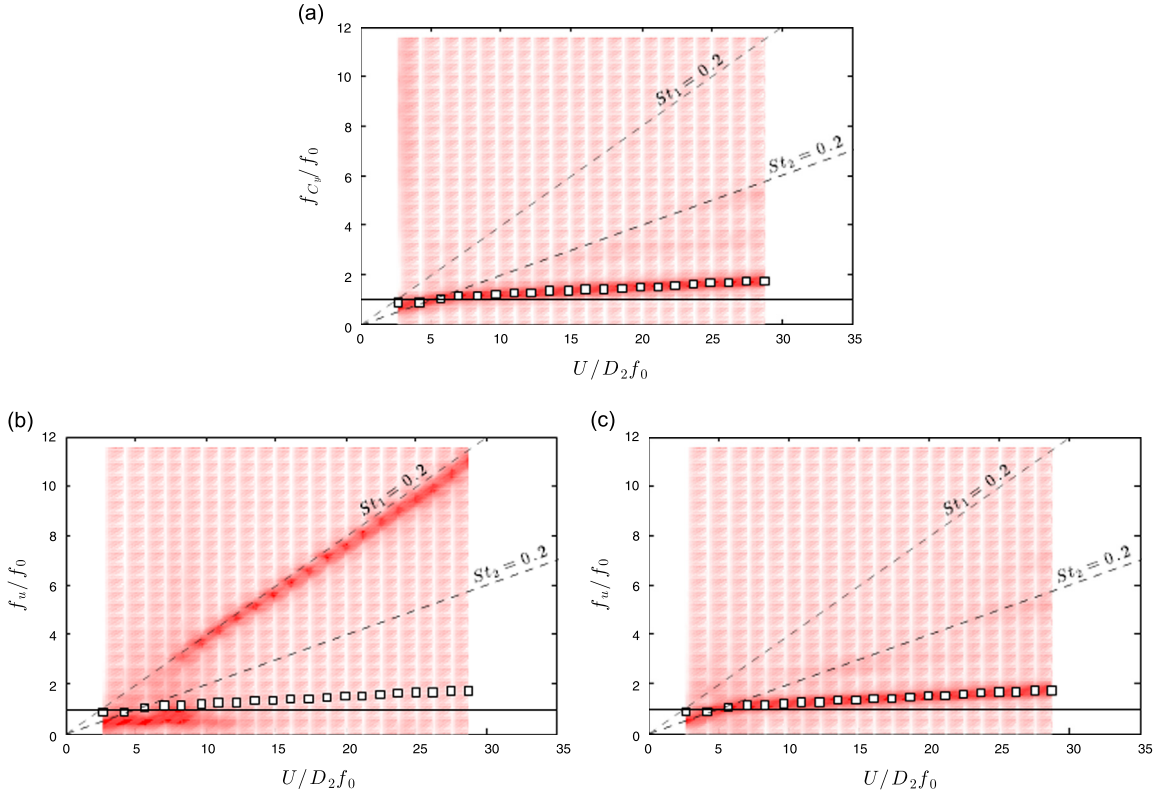

Fig. 5. Power spectra for configuration $D_1/D_2 = 1/2$. (a) Frequency of lift on the downstream cylinder. Frequency of velocity fluctuation in the wake of the (b) upstream and (c) downstream cylinders.

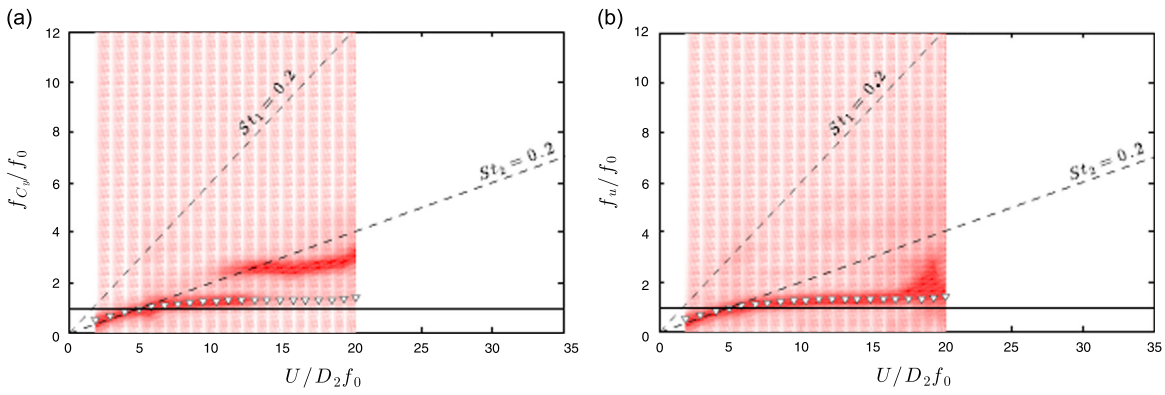

Fig. 6. Power spectra for configuration $D_1/D_2 = 1/3$. (a) Frequency of lift on the downstream cylinder and (b) frequency of velocity fluctuation in the wake of the downstream cylinder.

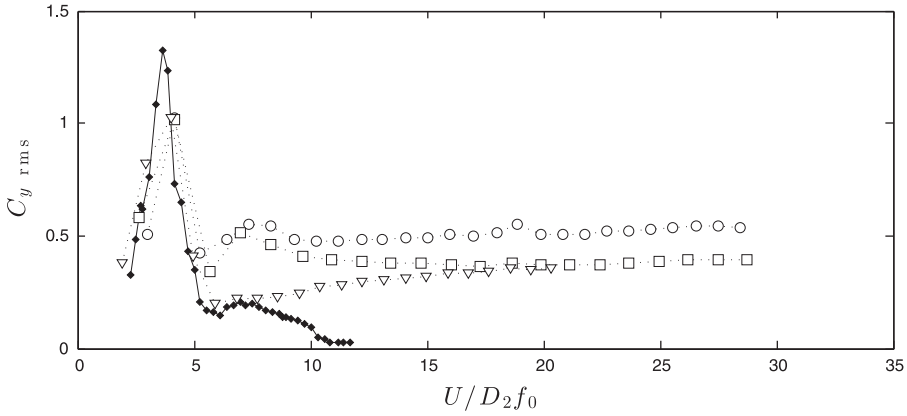

Fig. 7. Lift coefficient (r.m.s.) versus reduced velocity. Key: ◆, single cylinder VIV; ○, $D_1/D_2 = 1/1$; □, $D_1/D_2 = 1/2$; ▽, $D_1/D_2 = 1/3$.

Finally, for the $D_1/D_2 = 1/3$ configuration presented in Fig. 6(a) we observe that traces of the vortex shedding frequency of the upstream cylinder (occurring at $St_1 = 0.2$) are barely noticeable in the lift signature of the downstream cylinder. The lower branch associated with the frequency of vibration still dominates over the spectrum, however a second branch of $f_{C_y}/f_0 \approx 3$ appears for $U/D_2f_0 > 12$. It is not clear what mechanism this higher frequency represents. In the wake spectrum presented in Fig. 6(b) we do not observe other significant frequency branches other than the actual dominant frequency of vibration.

Based on the spectrum plots presented in Figs. 4–6 we conclude that the separation of S=200 mm (resulting in $L/D_1 = 3.5$, 7.0 and 6.5 for each respective configuration) was sufficiently large to prevent any interference from the downstream wake or vibration from propagating upstream to affect the vortex shedding mechanism of the first cylinder. The upstream cylinder behaved as an isolated static cylinder for all cases and the higher frequency associated with the upstream shedding reached the downstream cylinder and was captured by the lift spectrum for all cases. This is similar to what was observed by Huang and Sworn (2011) with the larger cylinder placed upstream. However, the vibration of the downstream body was not directly associated with that frequency of excitation, but it responded in a much lower frequency closely related to the frequency of wake stiffness (f_w) proposed by Assi et al. (2013).

3.2. Hydrodynamic force coefficients

In the response curves presented in Fig. 3 we observed that different levels of amplitude of vibration were reached by each D_1/D_2 case. We also noticed in the spectrum plots of Figs. 4–6 that the WIV excitation is indeed coming from the fully developed wakes of the upstream cylinders, which produce vortices with different strengths, lengths and time scales due to variations in D_1/D_2 and L/D_1. Now, in order to investigate how the amplitude of response is correlated with the upstream excitation we will turn to measurements of lift on the downstream cylinder.

Fig. 7 presents the r.m.s. of lift coefficient ($C_{y\ \mathrm{rms}}$) measured on the downstream cylinder compared with $C_{y\ \mathrm{rms}}$ measured on a single cylinder under VIV, the latter being in good agreement with the experimental data presented by Khalak and Williamson (1999). As expected, all tandem configurations present a peak of $C_{y\ \mathrm{rms}}$ corresponding to the local resonance of VIV at $U/D_2f_0 \approx 4$. After that, when $C_{y\ \mathrm{rms}}$ associated with VIV starts to diminish with the end of the synchronisation range,

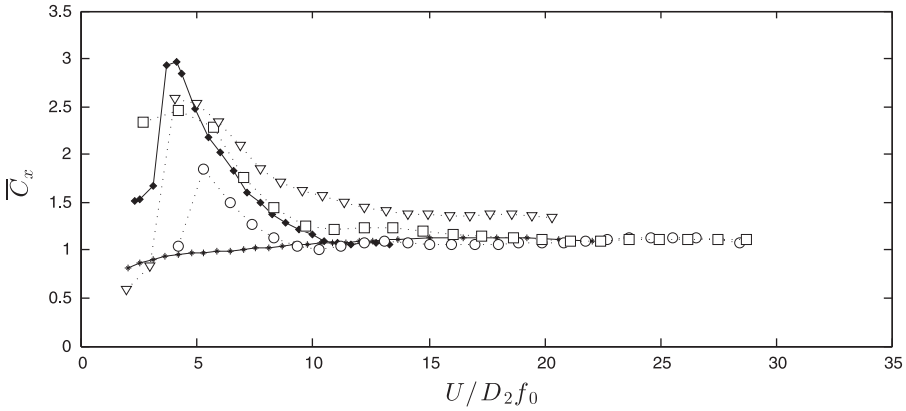

Fig. 8. Mean drag coefficient versus reduced velocity. Key: ∗, single static cylinder; ◆, single cylinder VIV; ○, $D_1/D_2 = 1/1$; □, $D_1/D_2 = 1/2$; ▽, $D_1/D_2 = 1/3$.

$C_{y\,\mathrm{rms}}$ for the tandem cases increases to a much higher level, which is sustained until the end of the reduced velocity range testes.

Lift coefficient for $D_1/D_2 = 1/1$ remains at $C_{y\,\mathrm{rms}} \approx 0.5$ while the other two cases find levels slightly below that, with $D_1/D_2 = 1/3$ showing the lowest $C_{y\,\mathrm{rms}}$ level. It appears that the level of $C_{y\,\mathrm{rms}}$ is more dependent on D_1/D_2 rather than on L/D_1. The amplitude of response ($\hat{y}/D_2$), on the other hand, seems to be more dependent on L/D_1 rather than on D_1/D_2, with $D_1/D_2 = 1/3$ reaching amplitudes higher than $D_1/D_2 = 1/2$. Nevertheless, as suggested before, this could also be related to the fact that $D_1/D_2 = 1/3$ presents half of the m^* of the other two cases.

We have seen that the lift on the downstream cylinder will act at the frequency of wake stiffness (f_w) and those of vortex shedding (f_s), which will be sustained for an indefinite range of reduced velocities during the WIV mechanism. Assi et al. (2010) explained how this excitation mechanism depends on the unsteady interaction of the vortices coming from the upstream wake and the downstream cylinder. Therefore, the topology of the wake (width, vortex strength, length, time scales, etc.) modified by an upstream cylinder of smaller diameter must be playing a fundamentally different role in the excitation mechanism.

Mean drag coefficients ($\overline{C}_x$) on the downstream cylinder are presented in Fig. 8. The drag curve for a single cylinder reveals the amplification of drag normally observed during the synchronisation range of VIV, which agrees well with the results presented by Khalak and Williamson (1999). A curve for the drag of a static single cylinder has also been added as a reference.

All tandem configurations present a similar amplification of drag during the resonance range of VIV. Past the synchronisation range, $\overline{C}_x$ due to WIV remains at slightly higher levels, but very close to the drag measured for a static single cylinder. In general, $\overline{C}_x$ decreases as D_1/D_2 increases, perhaps due to the deficit of mean velocity in the wake coming from the upstream cylinder; i.e. a smaller D_1 will create a wake with higher streamwise velocity reaching the second cylinder.

4. Conclusion

In the present work we investigate the WIV response of the downstream cylinder of a pair with diameter ratios $D_1/D_2 = 1/1$, 1/2 and 1/3. For all tandem configurations, the static upstream cylinder appears to be shedding vortices as an isolated cylinder, not being affected by the presence or movement of the downstream body. This is true for effective separations of $L/D_1 = 3.5$, 7.0 and 6.5, respectively.

The overall WIV response turned out to be dependent on several parameters: wake topology (Re), arrangement geometry (both D_1/D_2 and L/D_1) and system dynamics (m^*). Other dimensionless representations of the separation parameter can lead to different interpretations of the data. In the present work, the effective separation L/D_1 was chosen as a representative of the effect of the upstream wake impinging on the downstream body.

The frequency response, on the other hand, turned out to be rather independent of both D_1/D_2 and L/D_1. In fact, a mechanism similar to the wake stiffness proposed by Assi et al. (2013) might be occurring for different diameter ratios but with different intensities. Nevertheless, all frequency responses appeared to be very close to the wake stiffness frequency previously characterised for cylinders of equal diameters.

It is not clear from the present investigation if the enhanced response of $D_1/D_2 = 1/3$ in relation to $D_1/D_2 = 1/2$ is due to the decrease of the effective separation L/D_1, the decrease of m^* or the increase of Re. Assi et al. (2010) have already shown that Reynolds number plays a very important role in WIV. Maybe increasing the diameter of the downstream cylinder from 50 mm to 75 mm from case $D_1/D_2 = 1/2$ to 1/3 may include such a Re effect. Future experiments should be able to isolate some of these parameters in order to achieve a better understanding of the phenomenon.

Acknowledgements

The author is grateful to the advice of Prof. Peter Bearman and the support from Imperial College (Dept. of Aeronautics) and CAPES (2668-04-1) at the time of the experiments. He also wishes to acknowledge the recent support from FAPESP (2013/07335-8) and CNPq (308916/2012-3) that allowed him time to revisit the data and write this manuscript.

References

Alam, M.M., Zhou, Y., 2008. Strouhal numbers, forces and flow structures around two tandem cylinders of different diameters. Journal of Fluids and Structures 24, 505–526.

Alam, M.M., Zhou, Y., 2014. Flow-induced vibrations of a circular cylinder interacting with another of different diameter. In: Zhou, Y., Liu, Y., Huang, L., Hodges, D.H. (Eds.), Fluid–Structure–Sound Interactions and Control. Lecture Notes in Mechanical Engineering, Springer, Berlin, Heidelberg, pp. 385–390.

Assi, G.R.S., 2009. Mechanisms for Flow-Induced Vibration of Interfering Bluff Bodies (Ph.D. thesis). Imperial College London, London, UK, available from ⟨www.ndf.poli.usp.br/∼gassi⟩.

Assi, G.R.S., 2014. Wake-induced vibration of tandem and staggered cylinders with two degrees of freedom. Journal of Fluids and Structures, http://dx.doi.org/10.1016/j.jfluidstructs.2014.07.002, in press.

Assi, G.R.S., Bearman, P.W., Carmo, B., Meneghini, J., Sherwin, S., Willden, R., 2013. The role of wake stiffness on the wake-induced vibration of the downstream cylinder of a tandem pair. Journal of Fluid Mechanics 718, 210–245.

Assi, G.R.S., Bearman, P.W., Meneghini, J., 2010. On the wake-induced vibration of tandem circular cylinders: the vortex interaction excitation mechanism. Journal of Fluid Mechanics 661, 365–401.

Bearman, P.W., 1984. Vortex shedding from oscillating bluff bodies. Annual Review of Fluid Mechanics 16, 195–222.

Bokaian, A., Geoola, F., 1984. Wake-induced galloping of two interfering circular cylinders. Journal of Fluid Mechanics 146, 383–415.

Huang, S., Sworn, A., 2011. Some observations of two interfering VIV circular cylinders of unequal diameters in tandem. Journal of Hydrodynamics 23, 535–543.

Huang, S., Sworn, A., 2013. Interference between two stationary or elastically supported rigid circular cylinders of unequal diameters in tandem and staggered arrangements. J. Shore Mech. Arctic Eng. 135, 021803. (February 25, 2013) (10).

Khalak, A., Williamson, C.H.K., 1999. Motions, forces and mode transitions in vortex-induced vibrations at low mass-damping. Journal of Fluids and Structures 13, 813–851.

Rahmanian, M., Zhao, M., Cheng, L., Zhou, T., 2012. Two-degree-of-freedom vortex-induced vibration of two mechanically coupled cylinders of different diameters in steady current. Journal of Fluids and Structures 35, 133–159.

Ruscheweyh, H.P., 1983. Aeroelastic interference effects between slender structures. Journal of Wind Engineering and Industrial Aerodynamics 14, 129–140.

Tsutsui, T., Igarashi, T., Kamemoto, K., 1997. Interactive flow around two circular cylinders of different diameters at close proximity. Experiment and numerical analysis by vortex method. Journal of Wind Engineering and Industrial Aerodynamics 69–71, 279–291.

Williamson, C.H.K., Govardhan, R., 2004. Vortex-induced vibrations. Annual Review of Fluid Mechanics 36, 413–455.

Zdravkovich, M.M., 1988. Review of interference-induced oscillations in flow past two circular cylinders in various arrangements. Journal of Wind Engineering and Industrial Aerodynamics 28, 183–200.

Zhao, M., Cheng, L., Teng, B., Liang, D., 2005. Numerical simulation of viscous flow past two circular cylinders of different diameters. Applied Ocean Research 27, 39–55.

Zhao, M., Yan, G., 2013. Numerical simulation of vortex-induced vibration of two circular cylinders of different diameters at low Reynolds number. Physics of Fluids 25, 083601, ⟨http://dx.doi.org/10.1063/1.4816637⟩.